ACS APPLIED MATERIALS & INTERFACES

Letter

www.acsami.org

Porous Silicon Nanotube Arrays as Anode Material for Li-Ion Batteries

Alexander T. Tesfaye,[†,‡] Roberto Gonzalez,[§] Jeffery L. Coffer,[*,§] and Thierry Djenizian[*,†,‡,∥]

[†]Aix-Marseille University, CNRS, MADIREL Laboratory, UMR 7246, 13397 Marseille, France

[‡]FR CNRS 3104, ALISTORE-ERI, Nantes, France

[§]Department of Chemistry, Texas Christian University, Fort Worth, Texas 76129, United States

[∥]FR CNRS 3459, Réseau sur le Stockage Electrochimique de l'Energie (RS2E), Paris, France

Supporting Information

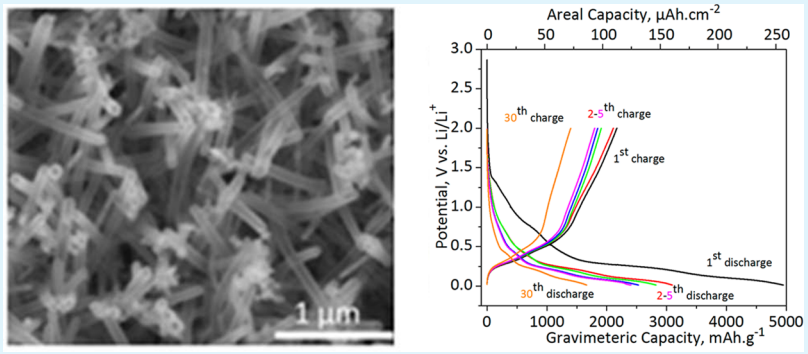

ABSTRACT: We report the electrochemical performance of Si nanotube vertical arrays possessing thin porous sidewalls for Li-ion batteries. Porous Si nanotubes were fabricated on stainless steel substrates using a sacrificial ZnO nanowire template method. These porous Si nanotubes are stable at multiple C-rates. A second discharge capacity of 3095 mAh g^{-1} with a Coulombic efficiency of 63% is attained at a rate of C/20 and a stable gravimetric capacity of 1670 mAh g^{-1} obtained after 30 cycles. The high capacity values are attributed to the large surface area offered by the porosity of the 3D nanostructures, thereby promoting lithium-ion storage according to a pseudocapacitive mechanism.

KEYWORDS: *silicon nanotube arrays, porous silicon, ZnO nanowire templates, anode, Li-ion batteries*

Currently, Li-ion batteries (LIBs) are the most studied energy storage systems because of the superior electrochemical performance in parameters such as high energy density, low self-discharge, and long cycle life.[1,2] Besides their application in electric vehicles, LIBs have become a significant energy storage system for microelectronic devices. However, the technology reaches a limit because of the low specific capacity offered by graphite (372 mA.h.g^{-1}), which is used as anode material. Because of a low operating potential (~0.25 V vs Li/Li^+) and the highest theoretical capacity reported so far (4200 mAh g^{-1}), Si is a promising negative electrode material for LIBs.[3−5] Si reacts reversibly with Li^+ by alloying/dealloying mechanisms according to eq 1.[6]

$$Si + xLi^+ + xe^- \leftrightarrows Li_xSi \text{ for } 0 \le x \le 4.4 \quad (1)$$

Unfortunately, the reaction is accompanied by large volume expansion (~400%), which results in pulverization and voltage cutoff in the first few cycles because of the loss of electrical contact.[7,8] To address this concern, one-dimensional nanomaterials such as nanowires, nanotubes, and nanoporous instead of bulk materials have been investigated. For example, the use of nanostructured materials like graphite and transitional metal oxides[9−11] have shown an improved electrochemical performance compared to their bulk counterpart. For Si-based anode materials, it has been reported that voids between nano-objects are beneficial in bearing the volume expansion during cycling,[12−16] which is otherwise responsible for the strong capacity fading and the poor electrochemical cycling obtained in the case of bulk Si.[7,17−19] The particular case of silicon nanotubes (SiNTs) offer well-defined uniform morphologies with a demonstrated impact on reversible capacity and long cycle life. Prior efforts have focused on sealed SiNTs (with or without carbon layers)[14,15] or rather large SiNTs (>400 nm diameter) containing porous silica shells.[20] In contrast, our group has recently developed methods for the fabrication of ultrathin (~10 nm) crystalline SiNTs with clearly defined porous sidewalls.[21] The morphology associated with this type of nanotube platform is in stark difference to the other nanotube morphologies examined previously, and warrants

Received: June 26, 2015
Accepted: September 9, 2015
Published: September 9, 2015

DOI: 10.1021/acsami.5b05705
ACS Appl. Mater. Interfaces 2015, 7, 20495−20498

investigation in terms of capacity retention and cycling performance.

In this work, the synthesis and electrochemical behavior of self-supported vertical porous SiNTs fabricated by using sacrificial ZnO nanowire array templates on stainless steel substrate are reported. We show that these self-supported SiNTs exhibit electrochemical properties to be of value as a negative electrode for LIBs.

The SiNTs were fabricated by a three-step template-directed method. First, the formation of a sacrificial ZnO nanowire template was carried out on stainless steel substrates. This involves initial deposition of a ZnO nanocrystal seed layer on stainless steel, followed by annealing at 300 °C. ZnO nanowire arrays were grown from these seed layers by a hydrothermal process at 95 °C using 0.02 M $Zn(NO_3)_2$ and 0.02 M hexamethylenetetramine as precursors. Then, deposition of Si onto the ZnO nanowires was performed using sample exposure to SiH_4 (0.5% in He) at 530 °C in a dilute He atmosphere. Finally, packed arrays of SiNTs were obtained by removal of the ZnO nanowire template in NH_4Cl vapor at 450 °C.[21] These SiNTs were characterized using a JEOL JSM 7100FT FE SEM as well as a JEM 2100 TEM with EDAX elemental analysis.

The electrochemical performance tests were carried out in two-electrode Swagelok assembled in a glovebox filled with purified argon in which moisture and oxygen content were less than 0.5 ppm. The half-cells consisted of as-formed self-standing SiNTs on stainless steel (0.55 cm^2) that were used as the working electrode and the current collector, respectively. A 9 mm diameter Li foil was used as the counter electrode and a Whatman glass microfiber separator soaked with lithium hexafluorophosphate in ethylene carbonate and diethylene carbonate (1 M $LiPF_6$ in (EC:DEC) 1:1 w/w) was used as separator. The mass of the active material was ~30 μg. The cyclic voltammetry and galvanostatic tests were done using a VMP3 potentiostat (Bio Logic, France). The cyclic voltammogram was performed in potential window of 0.01−1.75 V vs Li/Li^+ at a scan rate of 0.1 mV.s^{-1}. The galvanostatic tests of the assembled cells were done at multiple *C*-rates. *C*/*n* means the battery is fully charged or discharged up to its total storage capacity in *n* hours (for this work 1 *C* = 4.2 A g^{-1}). The gravimetric capacity values were calculated on the basis of the weight of the active material. For all electrochemical tests, additives and binders were not used.

The SiNTs were structurally characterized by a combination of field-emission SEM and TEM; the latter technique included high-resolution imaging along with in situ elemental energy dispersive X-ray analysis (EDX) (Figure 1). SEM imaging reveals dense packing of the nanotubes in a vertical fashion on the stainless steel substrate, as desired (Figure 1a). Complementary TEM analysis reveals a thin porous nature to the sidewalls of the nanotube, with a thickness on the order of 10 nm (Figure 1b). Pores on the order of 2−5 nm can be observed along the length of a given tube. Statistical analysis of inner tube diameter shows a mean value of 57 nm (± 11 nm) with corresponding lengths up to 2 μm. In terms of composition, EDX analysis detects only the presence of Si and some oxygen from surface oxide species (Figure 1c). The solid silicon regions of the nanotube are clearly crystalline in nature, as high magnification TEM imaging shows lattice spacings associated with the ⟨111⟩ index of cubic Si (Figure 1d).

Figure 2 shows the cyclic voltammogram (CV) recorded for first−fifth and 30th cycles. In agreement with previous

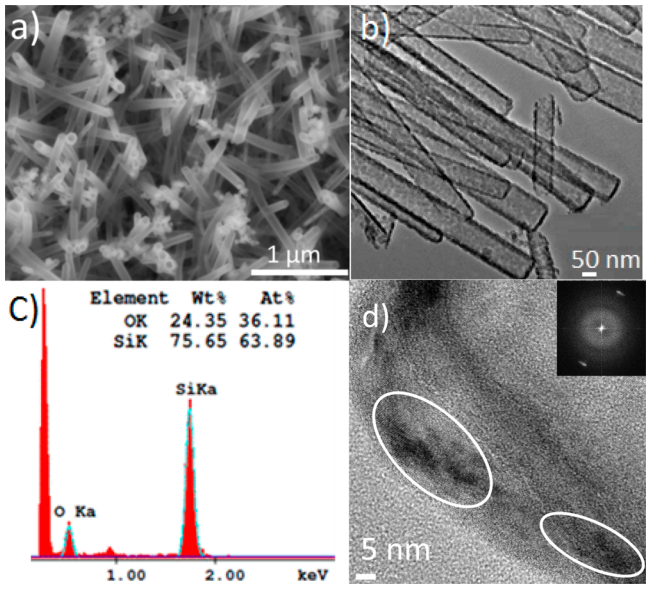

Figure 1. (a) Field-emission SEM image of SiNTs. (b) TEM of SiNTs. (c) EDX spectrum of SiNTs (from TEM analysis); small peak near 1.00 keV is associated with TEM sample grid. (d) HRTEM of SiNTs. White circles represent crystalline domains of ⟨111⟩ orientation; inset: FFT indicating sample crystallinity.

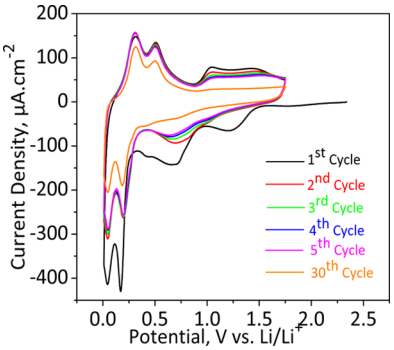

Figure 2. Cyclic voltammogram recorded for the SiNTs in the potential window of 0.01−1.75 V vs Li/Li^+ at the scan rate of 0.1 mV s^{-1}.

studies,[4,5] the electrochemical reactivity of the nanotubes are confirmed by the presence of four peaks during the first discharge. The irreversible peaks at 1.2 V vs Li/Li^+ are mainly due to the decomposition of the organic electrolyte leading to the formation of a solid electrolyte interface (SEI) at the surface of the electrode. The lithiation of the SiNTs begins around 0.4 V and further alloying is observed at 0.1 V vs Li/Li^+. The peaks at 0.38 and 0.5 V vs Li/Li^+ correspond to the dealloying of Si. The small broad peaks at potential of 0.7 and 1.0 V vs Li/Li^+ can be attributed to the reaction with iron oxide present in stainless steel substrate.[22] This material is known to demonstrate poor electrochemical behavior.[23,24]

Figure 3a shows the galvanostatic charge−discharge curves performed at C/20 for the SiNTs. In agreement with the CV curves for the first discharge, there are four small plateaus at potential of 1.2 V, 0.7 V, 0.4 and 0.1 V vs Li/Li^+ corresponding to the organic electrolyte decomposition, the reduction of Fe^{3+} to Fe^0 and the formation of Li_xSi. The first discharge capacity of 4950 mAh g^{-1} is obtained for the SiNTs. The second discharge capacity of 3095 mAh g^{-1} with a Coulombic efficiency of 63% is

DOI: 10.1021/acsami.5b05705
ACS Appl. Mater. Interfaces 2015, 7, 20495−20498

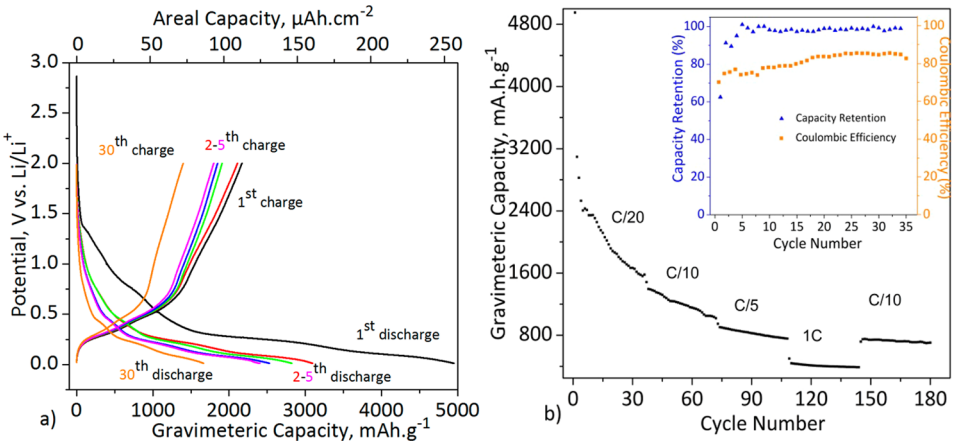

Figure 3. (a) Galvanostatic discharge−charge profile of SiNTs at *C*/20 and (b) their cycling performance at multiple *C*-rates. The inset shows the capacity retention and the Coulombic efficiency vs cycle number at *C*/20.

Table 1. Comparison of the Electrochemical Performance of Various SiNTs

working electrode	first discharge capacity (mAh g^{-1}) at *C*-rate	first irreversible capacity loss (%)	discharge capacity after (*n*) cycle (mAh g^{-1})	capacity retention (%) after (*n*) cycles	Coulombic efficiency (%) after (*n*) cycles
self-supporting SiNTs	4950 (0.05*C*)	63	1670 (30)	99.26 (30)	84.6 (30)
SiNTs[27]	1924 (0.5*C*)	80	1158 (10)	NA	60 (10)
SiNRs[26]	3285 (0.05*C*)	48.3	1398 (20)	NA	98.6 (20)
SiOC−CNT[28]	841.8 (0.1*C*)	67.1	686.3 (40)	81.5 (40)	99.6 (40)
carbon-coated SiNWs[29]	3344 (0.15*C*)	86	1326 (40)	NA	95 (40)
DW SiNTs[20]	1780 (0.2*C*)	99.9	1566 (6000)	> 99.9 (6000)	> 99.9 (6000)

attained. The capacity fading is attributed to the formation of the SEI layer and the irreversible reaction of Li^+ with iron oxide. Lithium ions react with iron oxide according to a conversion reaction mechanism to give metallic iron and Li_2O.[23,25] The formation of Li_2O is irreversible and is also responsible for the large capacity loss during the first cycle. Although the capacity values decrease further, a stable value around 1670 mAh g^{-1} can be observed after 30 cycles with capacity retention of 54%. These values are better than that reported for other selected Si nanostructured anodes,[26,27] but not as high as large double-walled SiNTs.[20] To place these results in the proper perspective, a comparison of the electrochemical performance of these SiNTs with previously reported literature results are shown in Table 1.

To study the operational stability of the SiNTs, the cycling life performance has been studied at multiple C-rates (Figure 3). At high current density (1*C*), a gravimetric capacity of 450 mAh g^{-1} is observed; when the *C*-rate is subsequently restored to a lower value (*C*/10), the capacity values reach 800 mAh g^{-1} suggesting that the microstructural features are partially preserved beyond 180 cycles (Figure S1). These results confirm that the porous three-dimensional geometry of the nanostructured Si electrode is beneficial to tolerating the large volume expansion during alloying/dealloying reactions. The inset in Figure 3b shows the capacity retention and the Coulombic efficiency. Apart from the first three cycles, a capacity retention of more than 97% has been observed, whereas the Coulombic efficiency of more than 75% has been obtained for the first few cycles. It should be noted that during cycling, the Coulombic efficiency increases slightly to reach 85% at the 30th cycle, but still remains lower than those obtained for double-walled SiNTs,[20] carbon-coated SiNTs,[29] and prelithiated SiNWs.[30]

The relatively high specific capacity value after 30 cycles and the excellent capacity retention of the SiNTs can be attributed to the high surface area of the porous nanotubular morphology.

The high surface to volume ratio offers more active sites for lithium storage owing to the larger electrode/electrolyte interface and promotes the storage of charges at the surface of the electrode according to a pseudocapacitive effect. This mechanism storage of charges can be verified by the presence of small plateaus and slopes in the charge/discharge profile.

To explain the origin of the capacity fading and the relatively low Coulombic efficiency, post-mortem SEM and EDS analysis were carried out (see Figures S1 and S2). EDS analysis revealed the presence of F, C, and O confirming the formation of a SEI layer. This effect could be avoided in principle by using a solid electrolyte. In addition, it can be observed that SiNTs are partially broken and detached from the substrate after cycling. Hence, the relative poor adhesion of nanotubes to the substrate leads to the loss of the electrical contact; in the future, this effect could be reduced by depositing a thin layer of Cr on stainless steel. Such a thin Cr layer could also be used to avoid the reaction of Li ions with iron oxide and the subsequent formation of Li_2O that also hinders electron transfer.

A ZnO nanowire sacrificial template method, in conjunction with dilute Si reactant concentrations, was used to fabricate vertical arrays of Si nanotubes with thin porous sidewalls. The as-grown self-supported nanostructures have been used as a working electrode in LIB-half-cell tests. The electrochemical characterizations revealed good, stable electrochemical performance that can be attributed to the morphological properties of the material. In spite of the large volume expansion and the

DOI: 10.1021/acsami.5b05705
ACS Appl. Mater. Interfaces 2015, 7, 20495−20498

SEI formation associated with the use of Si, 54% initial capacity is retained (1670 mAh g^{-1}) after 30 cycles and the capacity value of 800 mAh g^{-1} is attained after 180 cycles at C/10. With additional refinement of interfacial chemistry between nanotube and substrate, improvement of both capacity and efficiency is anticipated.

■ ASSOCIATED CONTENT

Supporting Information

The Supporting Information is available free of charge on the ACS Publications website at DOI: 10.1021/acsami.5b05705.

Post-mortem SEM and EDS data of SiNT anode materials (PDF)

■ AUTHOR INFORMATION

Corresponding Authors

*E-mail: thierry.djenizian@univ-amu.fr.

*E-mail: j.coffer@tcu.edu.

Notes

The authors declare no competing financial interest.

■ ACKNOWLEDGMENTS

We thank ALISTORE ERI and the Robert A. Welch Foundation (Grant P-1212 to JLC) for their financial support of this research.

■ REFERENCES

(1) Linden, D.; Reddy, T. *Handbook of Batteries*, 3rd ed.; McGraw−Hill: New York, 2001.

(2) Scrosati, B.; Garche, J. Lithium Batteries: Status, Prospects and Future. *J. Power Sources* **2010**, *195* (9), 2419−2430.

(3) Boukamp, B. A.; Lesh, G. C.; Huggins, R. A. All-Solid Lithium Electrodes with Mixed-Conductor Matrix. *J. Electrochem. Soc.* **1981**, *128* (4), 725−729.

(4) Chan, C. K.; Peng, H.; Liu, G.; McIlwrath, K.; Zhang, X. F.; Huggins, R. A.; Cui, Y. High-Performance Lithium Battery Anodes Using Silicon Nanowires. *Nat. Nanotechnol.* **2008**, *3* (1), 31−5.

(5) Liang, B.; Liu, Y.; Xu, Y. Silicon-Based Materials as High Capacity Anodes for Next Generation Lithium Ion Batteries. *J. Power Sources* **2014**, *267* (0), 469−490.

(6) Bogart, T. D.; Chockla, A. M.; Korgel, B. A. High Capacity Lithium Ion Battery Anodes of Silicon and Germanium. *Curr. Opin. Chem. Eng.* **2013**, *2* (3), 286−293.

(7) Kasavajjula, U.; Wang, C.; Appleby, A. J. Nano- and Bulk-Silicon-Based Insertion Anodes for Lithium-Ion Secondary Cells. *J. Power Sources* **2007**, *163* (2), 1003−1039.

(8) Beaulieu, L. Y.; Hatchard, T. D.; Bonakdarpour, A.; Fleischauer, M. D.; Dahn, J. R. Reaction of Li with Alloy Thin Films Studied by In Situ AFM. *J. Electrochem. Soc.* **2003**, *150* (11), A1457−A1464.

(9) Djenizian, T.; Hanzu, I.; Knauth, P. Nanostructured Negative Electrodes Based on Titania for Li-Ion Microbatteries. *J. Mater. Chem.* **2011**, *21* (27), 9925−9937.

(10) Ellis, B. L.; Knauth, P.; Djenizian, T. Three-Dimensional Self-Supported Metal Oxides for Advanced Energy Storage. *Adv. Mater.* **2014**, *26* (21), 3368−3397.

(11) Kyeremetang, N. A.; Plylahan, N.; Santos, A. C. S. D.; Traveira, L. V.; Dick, L. F. P.; Djenizian, T. Sulfidated TiO2 nanotubes: A potential 3D cathode material for Li-ion microbatteries. *Chem. Commun.* **2013**, *49*, 4205−4207.

(12) Zhou, X.-y.; Tang, J.-j.; Yang, J.; Xie, J.; Ma, L.-l. Silicon@Carbon Hollow Core−Shell Heterostructures Novel Anode Materials for Lithium Ion Batteries. *Electrochim. Acta* **2013**, *87* (0), 663−668.

(13) Jiang, J.; Li, Y.; Liu, J.; Huang, X. Building One-Dimensional Oxide Nanostructure Arrays on Conductive Metal Substrates for Lithium-Ion Battery Anodes. *Nanoscale* **2011**, *3* (1), 45−58.

(14) Park, M.-H.; Kim, M. G.; Joo, J.; Kim, K.; Kim, J.; Ahn, S.; Cui, Y.; Cho, J. Silicon Nanotube Battery Anodes. *Nano Lett.* **2009**, *9* (11), 3844−3847.

(15) Song, T.; Xia, J.; Lee, J.-H.; Lee, D. H.; Kwon, M.-S.; Choi, J.-M.; Wu, J.; Doo, S. K.; Chang, H.; Park, W. I.; Zang, D. S.; Kim, H.; Huang, Y.; Hwang, K.-C.; Rogers, J. A.; Paik, U. Arrays of Sealed Silicon Nanotubes as Anodes for Lithium Ion Batteries. *Nano Lett.* **2010**, *10* (5), 1710−1716.

(16) Wang, D.; Yang, Z.; Li, F.; Wang, X.; Liu, D.; Wang, P.; He, D. Performance of Si−Ni Nanorod as Anode for Li-Ion Batteries. *Mater. Lett.* **2011**, *65* (21−22), 3227−3229.

(17) Zhang, W.-J. A Review of The Electrochemical Performance of Alloy anodes for Lithium-Ion Batteries. *J. Power Sources* **2011**, *196* (1), 13−24.

(18) Simon, G.; Goswami, T. Improving Anodes for Lithium Ion Batteries. *Metall. Mater. Trans. A* **2011**, *42* (1), 231−238.

(19) Piper, D. M.; Yersak, T. A.; Lee, S.-H. Effect of Compressive Stress on Electrochemical Performance of Silicon Anodes. *J. Electrochem. Soc.* **2013**, *160* (1), A77−A81.

(20) Wu, H.; Chan, G.; Choi, J. W.; Yao, Y.; McDowell, M. T.; Lee, S. W.; Jackson, A.; Yang, Y.; Hu, L.; Cui, Y. Stable Cycling of Double-Walled Silicon Nanotube Battery Anodes through Solid-Electrolyte Interphase Control. *Nat. Nanotechnol.* **2012**, *7* (5), 310−315.

(21) Huang, X.; Gonzalez-Rodriguez, R.; Rich, R.; Gryczynski, Z.; Coffer, J. L. Fabrication and Size Dependent Properties of Porous Silicon Nanotube Arrays. *Chem. Commun.* **2013**, *49* (51), 5760−5762.

(22) Poizot, P.; Laruelle, S.; Grugeon, S.; Dupont, L.; Tarascon, J. M. Nano-Sized Transition-Metal Oxides as Negative-Electrode Materials for Lithium-Ion Batteries. *Nature* **2000**, *407* (6803), 496−499.

(23) Larcher, D.; Masquelier, C.; Bonnin, D.; Chabre, Y.; Masson, V.; Leriche, J.-B.; Tarascon, J.-M. Effect of Particle Size on Lithium Intercalation into α Fe2 O 3. *J. Electrochem. Soc.* **2003**, *150* (1), A133−A139.

(24) Ortiz, G. F.; Hanzu, I.; Lavela, P.; Tirado, J. L.; Knauth, P.; Djenizian, T. A Novel Architectured Negative Electrode Based on Titania Nanotube and Iron Oxide Nanowire Composites for Li-Ion Microbatteries. *J. Mater. Chem.* **2010**, *20* (20), 4041−4046.

(25) Reddy, M. V.; Subba Rao, G. V.; Chowdari, B. V. R. Metal Oxides and Oxysalts as Anode Materials for Li Ion Batteries. *Chem. Rev.* **2013**, *113* (7), 5364−5457.

(26) Zhou, Y.; Jiang, X.; Chen, L.; Yue, J.; Xu, H.; Yang, J.; Qian, Y. Novel Mesoporous Silicon Nanorod as an Anode Material for Lithium Ion Batteries. *Electrochim. Acta* **2014**, *127* (0), 252−258.

(27) Wen, Z.; Lu, G.; Mao, S.; Kim, H.; Cui, S.; Yu, K.; Huang, X.; Hurley, P. T.; Mao, O.; Chen, J. Silicon Nanotube Anode for Lithium-Ion Batteries. *Electrochem. Commun.* **2013**, *29* (0), 67−70.

(28) Bhandavat, R.; Singh, G. Stable and Efficient Li-Ion Battery Anodes Prepared from Polymer-Derived Silicon Oxycarbide−Carbon Nanotube Shell/Core Composites. *J. Phys. Chem. C* **2013**, *117* (23), 11899−11905.

(29) Huang, R.; Fan, X.; Shen, W.; Zhu, J. Carbon-Coated Silicon Nanowire Array Films for High-Performance Lithium-Ion Battery Anodes. *Appl. Phys. Lett.* **2009**, *95* (13), 133119.

(30) Liu, N.; Hu, L.; McDowell, M. T.; Jackson, A.; Cui, Y. Prelithiated Silicon Nanowires as an Anode for Lithium Ion Batteries. *ACS Nano* **2011**, *5* (8), 6487−6493.

DOI: 10.1021/acsami.5b05705
ACS Appl. Mater. Interfaces 2015, 7, 20495−20498